



Gestational/lactational tetrachlorobisphenol A exposure induces gut microbiota dysbiosis and metabolic disruption: Implications for intergenerational health risks

Yinfeng Zhou^{a,b,c}, Guoxia Zhang^d, Zenghua Qi^{a,b}, Zhaofa Huang^{a,b}, Yingxin Yu^{a,b,c,*}, Chaoyang Long^{c,**}

^a Guangdong-Hong Kong-Macao Joint Laboratory for Contaminants Exposure and Health, Guangdong Key Laboratory of Environmental Catalysis and Health Risk Control, Institute of Environmental Health and Pollution Control, Guangdong University of Technology, Guangzhou 510006, PR China

^b Guangdong Basic Research Center of Excellence for Ecological Security and Green Development, Key Laboratory of City Cluster Environmental Safety and Green Development, School of Environmental Science and Engineering, Guangdong University of Technology, Guangzhou 510006, PR China

^c Guangdong-Hong Kong-Macao Joint Laboratory for Contaminants Exposure and Health, Center for Disease Prevention and Control of Guangdong Province, Guangzhou 510430, PR China

^d Guangdong-Hong Kong-Macao Joint Laboratory for Contaminants Exposure and Health, Guangdong Provincial Key Laboratory of Tropical Disease Research, School of Public Health, Southern Medical University, Guangzhou 510515, PR China

ARTICLE INFO

Keywords:

Tetrachlorobisphenol A
Gut microbiota
Short-chain fatty acids
Metabolic pathway

ABSTRACT

Tetrachlorobisphenol A (TCBPA), a widely used chemical on material modification and flame retardant synthesis, bioaccumulates through the food chain and presents significant health concerns. However, the long-term effects of TCBPA exposure on gut microbial ecosystems and their metabolic functions remain poorly characterized. The present study developed a gestational/lactational exposure model in rats to systematically evaluate the impact on maternal and offspring gut microbiomes and fecal metabolomes by TCBPA exposure. 16S rRNA sequencing analysis demonstrated that TCBPA exposure significantly reduced both α -diversity indices and the relative abundance of critical short-chain fatty acid (SCFA)-producing genera, including *Lachnospiraceae*, *Ruminococcus*, *Lactobacillus*, and the unclassified *norank_o_Clostridia_UCG-014*. These results suggested that TCBPA perturbs gut microbiota by reducing key SCFA-producing bacteria. These microbial alterations were accompanied by corresponding decreases in fecal SCFA levels, indicating impaired microbial metabolic capacity. Metabolomics analysis revealed 18 metabolic pathways significantly affected by TCBPA, with the most marked changes in the arginine and proline metabolism pathway and the primary bile acid biosynthesis pathway. A strong correlation between gut microbiota and SCFA/metabolite levels suggests that alterations in gut microbiota may influence fecal metabolite metabolism. These findings collectively demonstrate that gestational/lactational TCBPA exposure induces persistent disruptions in gut microbial communities and their metabolic functions, which may underlie observed intergenerational health effects.

1. Introduction

Tetrachlorobisphenol A (TCBPA), a halogenated flame retardant, is extensively employed as an additive in electronics manufacturing, plastics production and synthetic textiles, with global annual production reaching 10,000 metric tons (Lei et al., 2024; Zhang et al., 2018). Owing to its environmental persistence, hydrophobicity, lipophilicity, and

bioaccumulation potential, TCBPA preferentially accumulates in lipid-rich tissues and biological fluids (Liu et al., 2023b). Notably, it has been found in human breast milk and corresponding embryos (Chen et al., 2015). Given the relatively closed nature of the uterine environment, maternal exposure is widely recognized as the main route for fetal contact (Chen et al., 2015). Early-life exposure to environmental pollutants, particularly during the fetal and infant stages, may alter gut

* Corresponding author at: Guangdong-Hong Kong-Macao Joint Laboratory for Contaminants Exposure and Health, Guangdong Key Laboratory of Environmental Catalysis and Health Risk Control, Institute of Environmental Health and Pollution Control, Guangdong University of Technology, Guangzhou 510006, PR China.

** Corresponding author.

E-mail addresses: yuyingxin@gdut.edu.cn (Y. Yu), chaoyang_long@163.com (C. Long).

<https://doi.org/10.1016/j.ecoenv.2026.120171>

Received 14 September 2025; Received in revised form 16 April 2026; Accepted 20 April 2026

Available online 23 April 2026

0147-6513/© 2026 The Author(s). Published by Elsevier Inc. This is an open access article under the CC BY-NC-ND license (<http://creativecommons.org/licenses/by-nc-nd/4.0/>).

microbial composition and contribute to long-term health risks (Liu et al., 2023a). However, studies have shown that TCBPA has various toxicities, including reproductive toxicity, genotoxicity, cytotoxicity, and neurotoxicity (Liu et al., 2023b; Zhang et al., 2018). Therefore, it is essential to evaluate the intergenerational effects of TCBPA.

The intestinal microbiota plays a fundamental role in maintaining gut ecosystem homeostasis and regulating crucial physiological processes (Lai et al., 2023; Lu et al., 2014). Moreover, substantial clinical and epidemiological studies have demonstrated strong correlations between gut dysbiosis and various diseases, including diabetes, hypertension, and fatty liver disease (Zhang et al., 2023; Hu et al., 2023). For instance, patients with pre-eclampsia exhibited significant reductions in beneficial genera such as *Faecalibacterium* and *Akkermansia*, while pathogenic bacteria (especially *Fusobacterium* and *Veillonella*) were significantly increased (Chen et al., 2020). Considering the pivotal role of gut microbiota in human pathophysiology and the established toxicity profile of TCBPA, there is a pressing need to investigate the potential impacts of the chemical on microbial community structure and function.

A primary function of the gut microbiota is the fermentation of dietary fibers to generate short-chain fatty acids (SCFAs), which serve as crucial energy substrates and metabolic regulators for the host (Xiao et al., 2023; Zhang et al., 2020). Emerging evidence suggests that dysregulated SCFA production may be associated with disease pathogenesis, including hypersensitivity disorders, carcinogenesis, and immune dysregulation (Xiao et al., 2023). However, the gut microbiota exhibits marked vulnerability to environmental stressors. Exposure to pollutants, antibiotics, or pathogens can induce dysbiosis (Lu et al., 2014), subsequently impairing intestinal barrier function and promoting inflammatory responses (Long et al., 2021; Tu et al., 2020). Of particular concern is the paucity of research on TCBPA-induced alterations in gut microbiota. Bisphenol A (BPA), a well-studied analog of TCBPA, has been extensively investigated for its effects on gut microbiota and related metabolic processes, including SCFA production and intergenerational outcomes (Reddivari et al., 2017; Zha et al., 2024). In contrast, despite its structural similarity to BPA and evidence suggesting potentially greater toxicity and endocrine-disrupting potential (Lei et al., 2024), its impacts on gut microbial equilibrium, microbiota–metabolite interactions, and maternal exposure-related intergenerational outcomes remain poorly understood.

Metabolic dysregulation resulting from gut microbial compositional shifts has been established as a critical contributor to disease pathogenesis (Chen et al., 2020; Lu et al., 2014). For instance, Chai et al. (2023) demonstrated that DEHP exposure interferes with gut microbial arachidonic acid metabolism, thereby increasing the risk of cardiovascular disease in obese mice. These findings underscore the importance of investigating TCBPA-associated metabolic perturbations mediated through gut microbiota alterations.

Therefore, this study hypothesizes that maternal TCBPA exposure disrupts gut microbial communities and metabolic homeostasis in both dams and offspring. To test this hypothesis, a TCBPA exposure model using pregnant Sprague-Dawley rats was established. The study mainly incorporated: (1) 16S rRNA sequencing to characterize TCBPA-induced gut microbiota alterations across generations; (2) GC-MS/MS quantification of fecal SCFAs; and (3) untargeted metabolomics to identify differentially expressed metabolites and perturbed metabolic pathways between the exposed and control groups. Furthermore, Spearman correlation analysis elucidated relationships between microbial shifts and SCFA/metabolite profiles. These results advance our understanding of intergenerational effects of TCBPA on gut microbiota composition and metabolic function, while providing critical toxicological insights into its potential long-term health risks.

2. Materials and methods

2.1. Standards and chemicals

Tetrachlorobisphenol A (TCBPA; CAS No. 79–95–8; purity >98.0%) was obtained from InnoChem Corporation (Beijing, China). All other reagents, including anhydrous calcium chloride, sulfuric acid, and diethyl ether, were obtained from Guangzhou Chemical Reagent Factory (Guangzhou, China). Complete chemical specifications are provided in [Supporting Information \(Text S1\)](#).

2.2. Animals and experimental design

Twenty-four sexually mature male and forty-eight nulliparous female Sprague-Dawley (SD) rats were acquired from the Experimental Animal Center of Southern Medical University. Animals were housed under standardized conditions: ambient temperature maintained at 22–26 °C, 12:12 h light-dark cycle, and relative humidity of 40–60%, with ad libitum access to standard rodent chow and filtered water. Following a 7-day acclimation period, breeding pairs were established at a 2:1 female-to-male ratio (3 rats/cage). Cohabitation occurred daily from 18:00–08:00 h. Successful mating was confirmed by microscopic identification of sperm and/or vaginal plugs, with the detection day designated as gestational day 0 (GD0). Confirmed pregnant dams were subsequently single-housed under controlled environmental conditions.

Pregnant dams were randomly allocated to six experimental groups ($n = 8$ per group), comprising three TCBPA-treated groups and three matched vehicle controls. The TCBPA exposure protocol consisted of: (1) continuous 42-day exposure followed by post-lactation dissection; (2) 21-day exposure with termination at lactation completion; and (3) 21-day exposure with prenatal termination. The exposure durations (21 and 42 days) were selected to reflect key reproductive stages in rats, corresponding to gestation and gestation plus lactation, respectively. Control animals received equivalent volumes of corn oil via oral gavage. The TCBPA dosage (100 mg/kg) was selected based on established toxicological studies, corresponding to approximately 1/60 of the oral LD₅₀ in rats and representing a sublethal exposure level commonly used to evaluate biological effects (Lei et al., 2024). This dose has been reported to induce endocrine and physiological alterations in rodents, supporting its use for evaluating potential biological effects (Lei et al., 2024). Based on allometric scaling (Nair and Jacob, 2016; Yao et al., 2024), this dose corresponds to a human equivalent dose (HED) of approximately 16.2 mg/kg. Detailed group nomenclature and sacrifice timepoints are provided in [Table 1](#), [Text S2](#) and [Fig. S1](#).

In this study, the multiple time points for fecal sample collection included the late gestation and late lactation periods of the dams, along with the immature (4-week-old) and adult (8-week-old) stages in offspring. Both control and TCBPA-exposed groups were humanely euthanized at corresponding time points. To minimize potential confounding effects of age, body size, and developmental timing, all statistical and omics analyses were conducted within each developmental stage (i.e., dams, 4-week-old offspring, and 8-week-old offspring), rather than across stages. All experimental procedures were approved by the Ethics Review Committee of Southern Medical University (SMUL202403028).

2.3. Gut microbiota analysis

Genomic DNA was extracted from fecal samples using the FastPure Stool DNA Isolation Kit (MJYH, Shanghai, China). DNA concentration and purity were measured using a NanoDrop 2000 UV-Vis spectrophotometer (Thermo Scientific, Wilmington, USA). The V3–V4 hypervariable regions of the 16S rRNA gene were amplified via PCR using the primers 338 F (5'-ACTCCTACGGGAGGCAGCAG-3') and 806 R (5'-GGACTACHVGGGTWTCTAAT-3'). Detailed bioinformatics analysis methods are provided in [Supporting Information \(Text S3\)](#).

Table 1

Summary of maternal exposure and offspring sampling design (n = 8). Note: ✓ indicates exposure during the corresponding period. GD21 and LD21 represent gestation day 21 and lactation day 21, respectively. 4 W and 8 W indicate offspring sampled at 4 and 8 weeks of age.

Group (dams)	Treatment	Exposure (Gestation)	Exposure (Lactation)	Euthanasia (day)	Offspring
CO1	Corn oil	✓	✓	LD21	4 W (CO1_4W), 8 W (CO1_8W)
CO2	Corn oil	✓	–	LD21	4W (CO2_4W), 8W (CO2_8W)
CO3	Corn oil	✓	–	GD21	–
EP1	TCBPA (100 mg/kg)	✓	✓	LD21	4 W (EP1_4W), 8 W (EP1_8W)
EP2	TCBPA (100 mg/kg)	✓	–	LD21	4 W (EP2_4W), 8 W (EP2_8W)
EP3	TCBPA (100 mg/kg)	✓	–	GD21	–

2.4. Sample treatment

The SCFA extraction from fecal samples followed previously reported methods (Zhang et al., 2023), with details in Supporting Information (Text S4). For untargeted metabolomics, published analytical approaches (Chai et al., 2023) with some modifications were adapted. Specifically, each 50 mg fecal aliquot was homogenized with 1 mL of ice-cold extraction solvent (water:methanol:acetonitrile, 1:2:2, v/v/v) containing 4-chlorophenylalanine as internal standard. Comprehensive sample preparation procedures for metabolomics are documented in Text S5.

2.5. Instrumental analysis

The quantification of SCFAs was conducted using a Shimadzu GC-MS/MS system (triple quadrupole) operating in selected ion monitoring (SIM) mode, which was exclusively used for the targeted quantification of fecal SCFAs in this study. The analytical separation employed an HP-FFAP capillary column (30 m × 0.25 mm, 0.25 μm film thickness) with a free fatty acid-optimized stationary phase. Helium carrier gas was maintained at a constant flow rate of 1.0 mL/min. Detailed instrumental parameters are described in Text S6.

Untargeted metabolomic profiling was conducted using a Thermo Scientific Ultimate 3000 UHPLC system coupled with a Waters HSS T3 column (2.1 mm × 100 mm, 1.8 μm particle size), which was used for untargeted metabolomic profiling. Chromatographic separation was performed under the following conditions: 25 min analytical run time, 10 μL injection volume, 0.3 mL/min flow rate, and isothermal column temperature maintenance at 30 °C. Complete system configuration details are documented in Text S7.

2.6. Quality assurance and quality controls

To ensure analytical reliability, quality assurance procedures were implemented through recovery efficiency evaluation using matrix-spiked samples containing known concentrations of target analytes. All reported concentrations were recovery-corrected. For SCFAs, matrix spike recoveries ranged from 75.0% to 122.7%. Quantification was performed using calibration curves demonstrating excellent linearity ($R^2 > 0.99$ for all curves). Method sensitivity was established with limits

of detection (LOD) and quantification (LOQ) defined as signal-to-noise ratios of 3:1 and 10:1, respectively. Detailed results are provided in Table S1.

2.7. Statistical analysis

Sample size (n) is provided in figure captions and table notes. Data were presented as means and standard deviations. One-way analysis of variance (one-way ANOVA) was performed using SPSS v25.0 (IBM, Chicago, IL), followed by Tukey's multiple comparison test to evaluate differences among groups, with significance defined as $p < 0.05$. Prior to analysis, data normality and homogeneity of variance were assessed using the Shapiro-Wilk test and Levene's test, respectively. Figures were generated using GraphPad Prism 10.0. A volcano plot for metabolomic analysis was generated using Origin 2025. To evaluate intergroup variations, PLS-DA was conducted with SIMCA-P 14.1. MetaboAnalyst 6.0 (<https://www.metaboanalyst.ca>) was used to analyze the metabolic pathways of the identified metabolites.

3. Results and discussion

3.1. Influence of TCBPA exposure on host growth parameters

Immature offspring in the EP1_4W group demonstrated significantly lower body weights compared to controls (CO1_4W) (Fig. 1A), whereas the EP2_4W group showed elevated body weights but markedly reduced small intestine length relative to controls (CO2_4W) (Fig. 1A, C). No significant differences were observed in large intestine length among groups in 4-week-old offspring (Fig. 1B). Notably, EP1_4W offspring displayed significantly lower body weights but higher small intestine weights compared to EP2_4W (Fig. 1A, G). In adulthood, EP1_8W offspring maintained significantly greater body and kidney weights than CO1_8W controls (Fig. 1D, H). These results demonstrate that TCBPA exposure induces exposure-pattern-dependent growth effects, with continuous gestational and lactational exposure leading to persistent phenotypic alterations. Similar to the present findings, exposure to low-dose BPA (0.1 mg/kg) during pregnancy and lactation in dams has been shown to induce persistent increases in offspring body weight that continue into adulthood (Rubin et al., 2001). In contrast, no significant differences were observed between EP2_8W and CO2_8W groups in body weight (Fig. 1D), intestine length (Fig. 1E-F), and all measured organ weights (Fig. 1H). This reversible effect indicates that the lactational period is a critical window for sustained TCBPA growth toxicity, as gestational-only exposure effects can be compensated during postnatal development. In general, the observed phenotypic differences attenuated progressively from late lactation through adulthood.

3.2. Influence of TCBPA exposure on gut microbiota diversity

α-Diversity metrics, including the Chao index (microbial richness) and Shannon index (community diversity), revealed significant TCBPA exposure effects (Fig. 2A, B). In dams, all exposed groups (EP1-EP3) demonstrated reduced α-diversity (Chao and Shannon indices) compared to matched controls, indicating compromised microbial richness and diversity. Immature offspring in the EP1_4W group showed reduced α-diversity relative to CO1_4W controls. This reduction persisted into adulthood in EP1_8W and EP2_8W groups, suggesting long-term dysbiosis following maternal TCBPA exposure. However, EP2_4W immature offspring exhibited elevated Chao and Shannon indices compared to CO2_4W controls, potentially reflecting microbial community recovery after cessation of TCBPA exposure during lactation.

Comparative analysis revealed significant exposure-duration effects on microbial diversity. Dams in the EP1 group (gestational+lactational exposure) exhibited lower Chao1 and Shannon indices than EP2 dams (gestational-only exposure). This pattern persisted in offspring, with EP1_4W immature offspring showing significantly reduced α-diversity

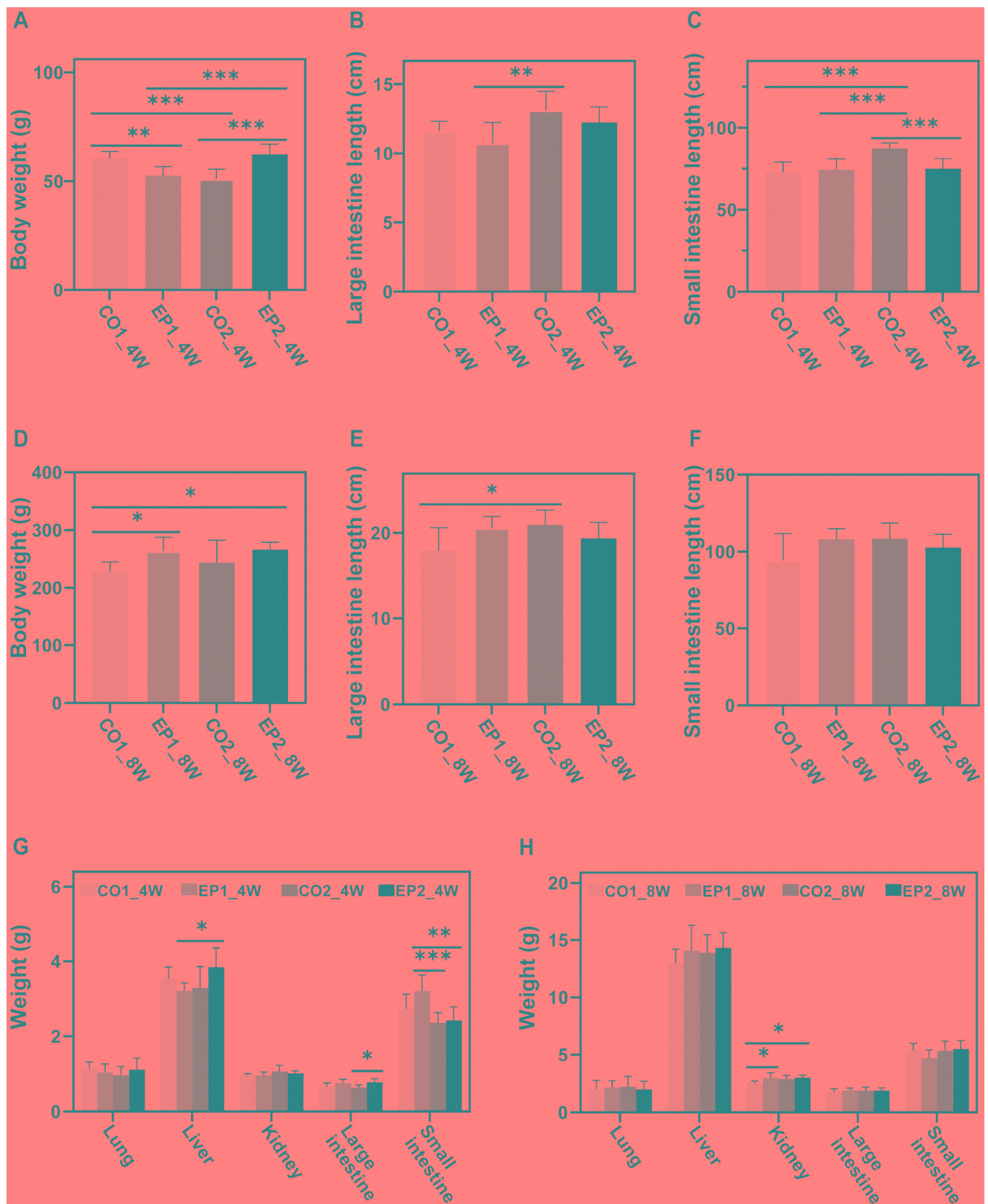


Fig. 1. Influence of TCBCPA exposure on growth parameters in offspring (n = 8). Body weight before sacrifice in offspring (A, D); Large intestine length (B, E); Small intestine length (C, F); Weights of organs in immature (G) and adult offspring (H). (Data presented as means ± SD. * $p < 0.05$, ** $p < 0.01$, *** $p < 0.001$ indicate significant differences between the indicated groups).

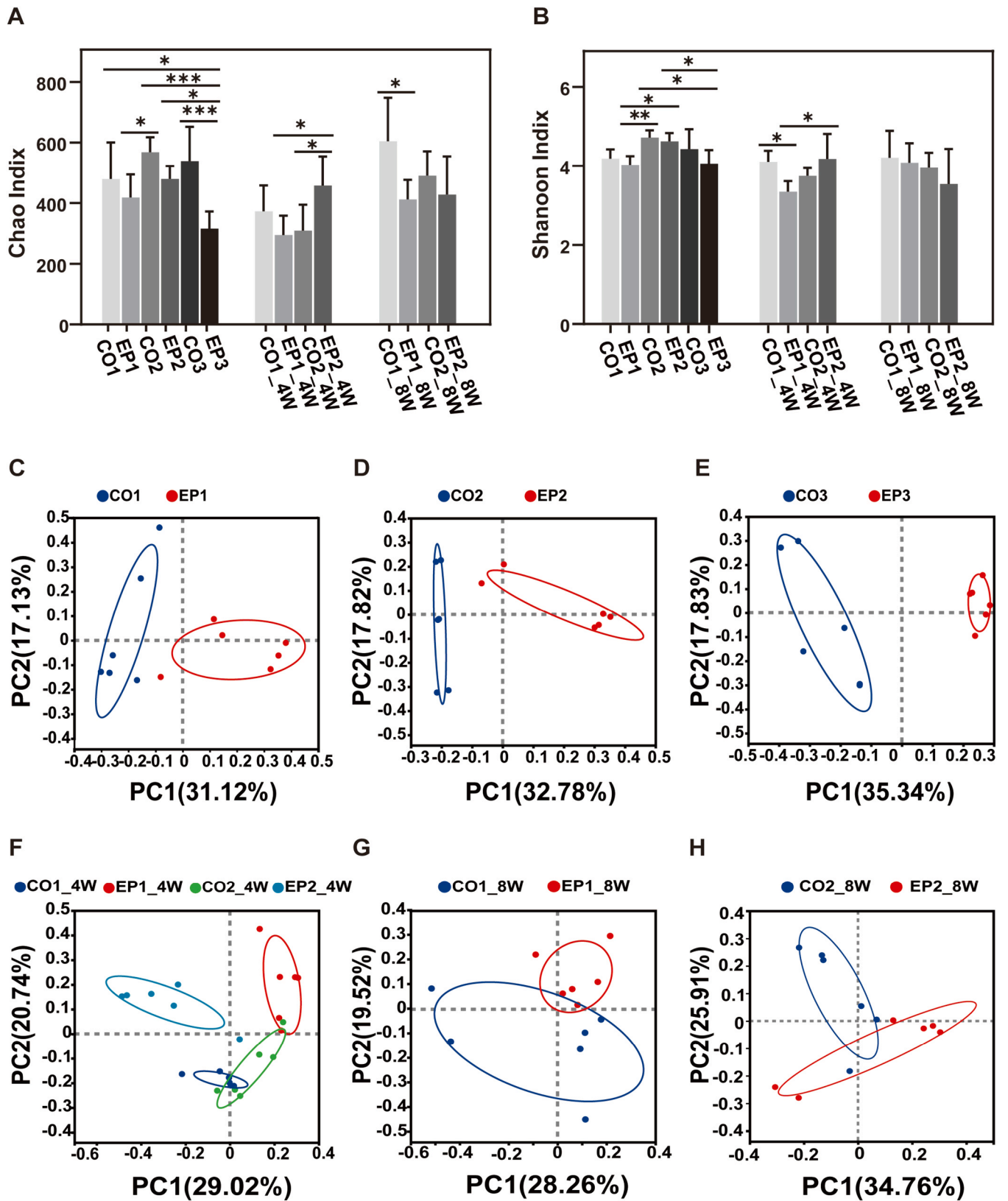


Fig. 2. Influence of TCBPA on the diversity in gut microbiota (n = 6). Chao index of α -diversities (A); Shannon index of α -diversities (B); PCoA of β -diversities in maternal rats (C-E); PCoA plots of β -diversities in offspring (F-H). (Data presented as means \pm SD. * $p < 0.05$, ** $p < 0.01$, *** $p < 0.001$ indicate significant differences).

compared with EP2_4W, and EP1_8W adults demonstrating lower Chao richness than EP2_8W (Fig. 2A). These findings suggest dose-duration dependent microbial dysbiosis with potential intergenerational transmission. Additionally, EP2 dams showed higher Shannon diversity than EP3 dams (gestational exposure followed by immediate euthanasia) (Fig. 2B), further indicating partial microbial community recovery following exposure cessation. Collectively, maternal TCBCPA exposure consistently reduced microbial diversity in both dams and offspring.

Similar to our findings, Liu et al. (2023a) observed a decreased α -diversity in both dams and offspring after resorcinol-bis (diphenyl)-phosphate exposure. Our previous studies indicated that environmental contaminants may interfere with gut microbiota balance, reduce microbial diversity, and consequently compromise host health (Zhang et al., 2020). The observed α -diversity reductions in our study suggest that maternal TCBCPA exposure may similarly impair gut microbial ecosystem stability across generations.

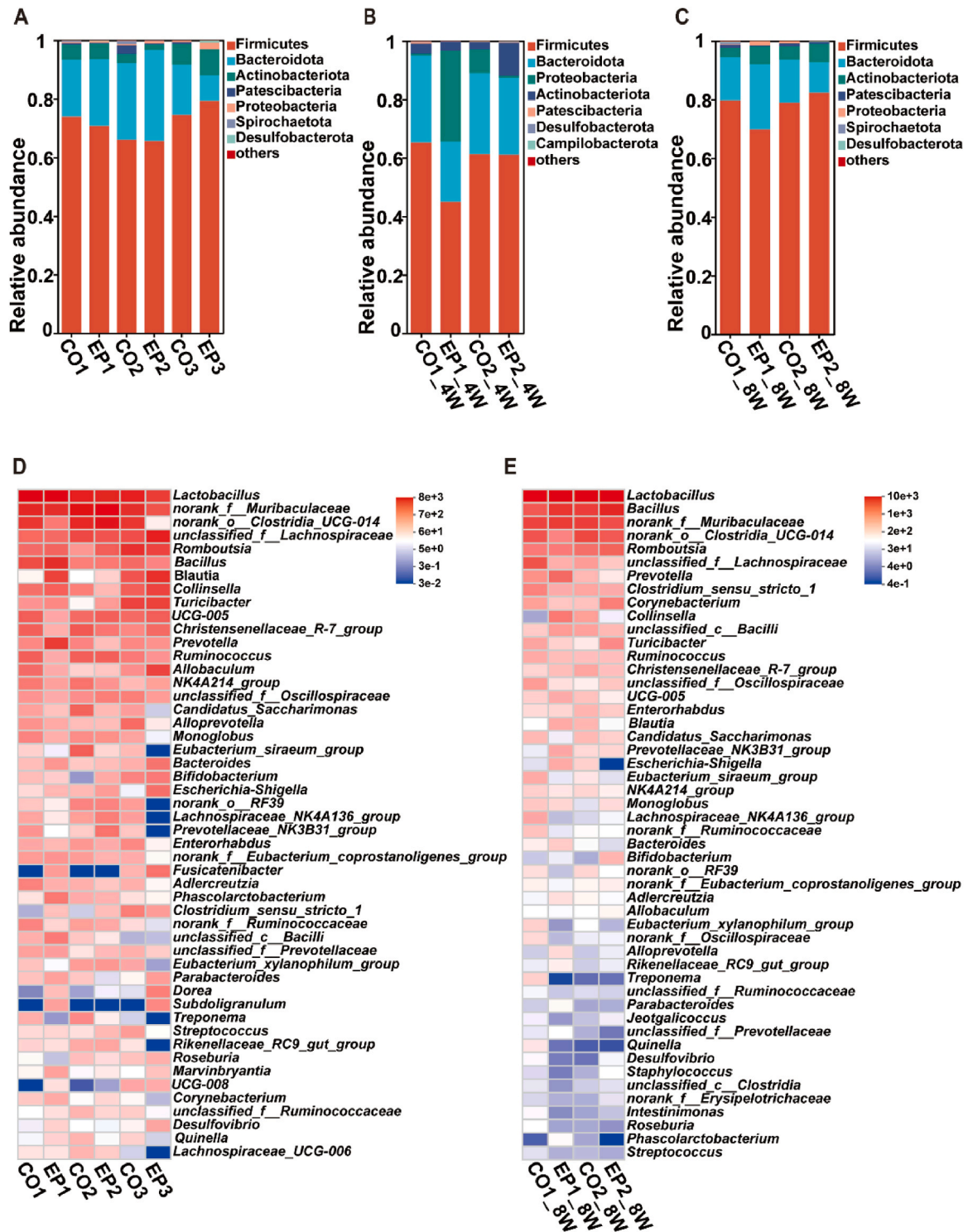


Fig. 3. Gut microbiome alterations induced by TCBCPA exposure (n = 6). Composition of the gut microbiota at the phylum level in dams (A), immature offspring (B), and adult offspring (C) (n = 6); Heatmaps of the relative abundance at the genus level in dams (D) and adult offspring (E).

The PCoA plots demonstrated clear segregation between control and TCBPA-exposed groups for both dams (Fig. 2C-E) and immature offspring (Fig. 2F), indicating significant exposure-induced perturbations in gut microbial architecture. However, adult offspring exhibited partial clustering overlap between exposure and control groups (Fig. 2G, H), suggesting age-dependent microbial community resilience following developmental TCBPA exposure.

Integrating results from α - and β -diversity, these findings demonstrated that maternal TCBPA exposure during gestation and/or lactation induced persistent gut microbial dysbiosis that extends to offspring. While partial microbial recovery occurred post-exposure, early-life perturbations may exert lasting developmental consequences. These findings underscore the particular vulnerability of the perinatal period to environmental disruption of microbial ecosystems.

3.3. Influence of TCBPA exposure on gut microbiota composition

At the phylum level, the gut microbiota in fecal samples was dominated by *Firmicutes* and *Bacteroidota* (Fig. 3A-C). *Firmicutes* levels were reduced in EP1 and EP2 dams and their immature offspring compared to controls (Fig. 3A-B), whereas it increased in the EP3 dams. *Bacteroidota* exhibited an opposing trend, increasing in EP1 but decreasing in EP3 dams relative to controls (Fig. 3A). In adult offspring, *Actinobacteriota* abundance was elevated in both EP1_8W and EP2_8W groups (Fig. 3C). Notably, *Bacteroidota* demonstrated progressive depletion across generations in the EP1 lineage, declining from 31% in dams to 26% in immature offspring and 10% in adults (Fig. 3A-C). The *Firmicutes/Bacteroidota* ratio is a crucial factor in maintaining gut microbial stability, and its dysregulation is associated with dysbiosis, which may heighten disease susceptibility (Zhang et al., 2023).

At the genus level, heatmap analysis revealed significant alterations in gut microbiota composition among TCBPA-exposed dams and their offspring. In exposed dams, we observed decreased relative abundances of *Lactobacillus*, *Ruminococcus*, and *norank_f_Ruminococcaceae*, alongside increased levels of *Escherichia-Shigella* (Fig. 3D). The reduction of *Lactobacillus* (a beneficial bacterium) is particularly noteworthy given its demonstrated role in reducing adipocyte size and regulating weight gain in high-fat diet models (Li et al., 2016). Similarly, the diminished abundance of fiber-degrading *Ruminococcus*, which contributes to acetate and formate production, and *norank_f_Ruminococcaceae* (observed across both exposed dams and adult offspring; Fig. 3D-E) may impair butyrate synthesis - a process critically linked to anti-inflammatory responses and mucosal integrity (Baltazar-Díaz et al., 2022; Zhuang et al., 2019). Conversely, the elevated *Escherichia-Shigella* levels could compromise intestinal barrier function.

In immature offspring, TCBPA exposure induced significant alterations in gut microbial composition, characterized by increased relative abundances of *Alloprevotella*, *Rikenellaceae_RC9_gut_group*, *Dubosiella*, *Corynebacterium*, alongside decreased levels of *Bacteroides* (Fig. S2). Notably, *Alloprevotella* enrichment has been associated with spleen-deficiency-induced diarrhea in rats, potentially exacerbating intestinal barrier dysfunction and abdominal symptoms (Shi et al., 2019). Similarly, *Rikenellaceae_RC9_gut_group* expansion correlates with colitis progression and purine metabolism disruption in dextrose sodium sulfate-induced colitis models (Li et al., 2024b), while *Dubosiella* proliferation demonstrates positive associations with intestinal inflammation and oxidative stress (Lin et al., 2022). Although typically commensal, *Corynebacterium* may act as an opportunistic pathogen in immunocompromised hosts, exhibiting both virulence and antibiotic resistance (Dragomirescu et al., 2020). In contrast, *Bacteroides* demonstrates dual beneficial effects, exhibiting both anti-inflammatory properties and metabolic regulatory functions (Wei et al., 2022).

In adult offspring, TCBPA exposure reduced the relative abundance of key beneficial taxa including *unclassified_f_Lachnospiraceae*, *Roseburia*, *Quinella*, and *norank_o_Clostridia_UCG-014* (Fig. 3E). Several members of the *unclassified_f_Lachnospiraceae* family, such as *Roseburia*,

contribute to SCFA biosynthesis and enhance host immunity against pathogens (Liu et al., 2023a), while *Quinella* generates essential metabolites (lactate, acetate, propionate) that support digestive health (Gruninger et al., 2014). The observed depletion of *Roseburia* may dysregulate metabolic pathways associated with irritable bowel syndrome pathogenesis (Dai et al., 2022), whereas reduced *norank_o_Clostridia_UCG-014* could impair intestinal repair mechanisms mediated through immune modulation (Li et al., 2024a). Additionally, emerging evidence implicates the correlation of multiple *Treponema* species with the etiology and pathogenicity of interdigital dermatitis (Beninger et al., 2018), highlighting the broader implications of TCBPA-induced microbial shifts. These findings suggest that TCBPA may indirectly compromise host health through persistent modulation of gut microbial communities.

3.4. Effect of TCBPA exposure on metabolism of SCFAs in gut microbiota

To assess TCBPA-induced perturbations in gut microbial metabolic function, seven fecal SCFAs (acetate, propionate, isobutyrate, butyrate, isovalerate, valerate, and caproate) were quantified. As shown in Fig. 4A and B, acetate, propionate, and butyrate constituted the predominant SCFAs across all groups, maintaining a consistent concentration gradient (acetate > propionate > butyrate). Differences were evaluated within each developmental stage to ensure comparability. Comparative analysis revealed significantly reduced SCFA levels in TCBPA-exposed dams and offspring relative to controls (Fig. 4A-E; Fig. S3). However, the EP2_4W immature group demonstrated elevated SCFA concentrations compared to CO2_4W controls. Among exposure groups, EP2 dams exhibited markedly higher SCFA levels than EP1 and EP3 dams. This pattern persisted in offspring, with EP2_4W immature offspring showing significantly increased SCFA versus EP1_4W, and EP2_8W adults displaying higher concentrations of all SCFAs except for butyrate compared to EP1_8W. Notably, these SCFA fluctuations paralleled α -diversity changes, particularly the Shannon index (Fig. 2A, B). Reduced Shannon diversity indicated impaired microbial function, contributing to decreased SCFA production and highlighting its sensitivity as an indicator of TCBPA-induced toxicity. Overall, SCFA levels varied across developmental stages and exposure windows under the same dose condition.

To examine the relationship between microbial dysbiosis and SCFA alterations, Spearman correlation analysis was performed between SCFA levels and differential genera identified by LEfSe (LDA >3, $p < 0.05$) (Fig. 4F). The present results demonstrated that reduced fecal SCFA levels were strongly correlated with depletion of key SCFA-producing taxa, including *Lachnospiraceae* (Liu et al., 2023a), *Ruminococcus* (Baltazar-Díaz et al., 2022), *Lactobacillus* (Chen et al., 2023), and *norank_o_Clostridia_UCG-014* (Lai et al., 2023). Specifically, the present results showed that *Lachnospiraceae* was positively associated with valerate, butyrate, propionate, and acetate; *Ruminococcus* was positively correlated with all seven SCFAs; *Lactobacillus* was positively linked to isovalerate and isobutyrate; and *norank_o_Clostridia_UCG-014* showed robust positive correlations with all SCFAs ($p < 0.001$). The observed reduction of these taxa in TCBPA-exposed groups suggested their critical role in SCFA biosynthesis impairment. Notably, *Alloprevotella*, an SCFA-producing genus (Wang et al., 2020), showed negative (non-significant) correlations with all SCFAs, and its enrichment in exposed offspring may contribute to reduced SCFA production. Conversely, the pathogenic *Escherichia-Shigella* demonstrated a significant negative correlation with all SCFAs ($p < 0.001$), consistent with its elevated abundance in TCBPA-exposed dams. Similarly, its elevated abundance in alcohol-decompensated cirrhosis was associated with a significant reduction in fecal SCFA levels and diminished microbial pathways for SCFA synthesis (Baltazar-Díaz et al., 2022). These findings collectively indicate that TCBPA exposure disrupts microbial ecosystems, primarily through depletion of beneficial SCFA producers.

Short-chain fatty acids play an essential role in metabolic regulation,

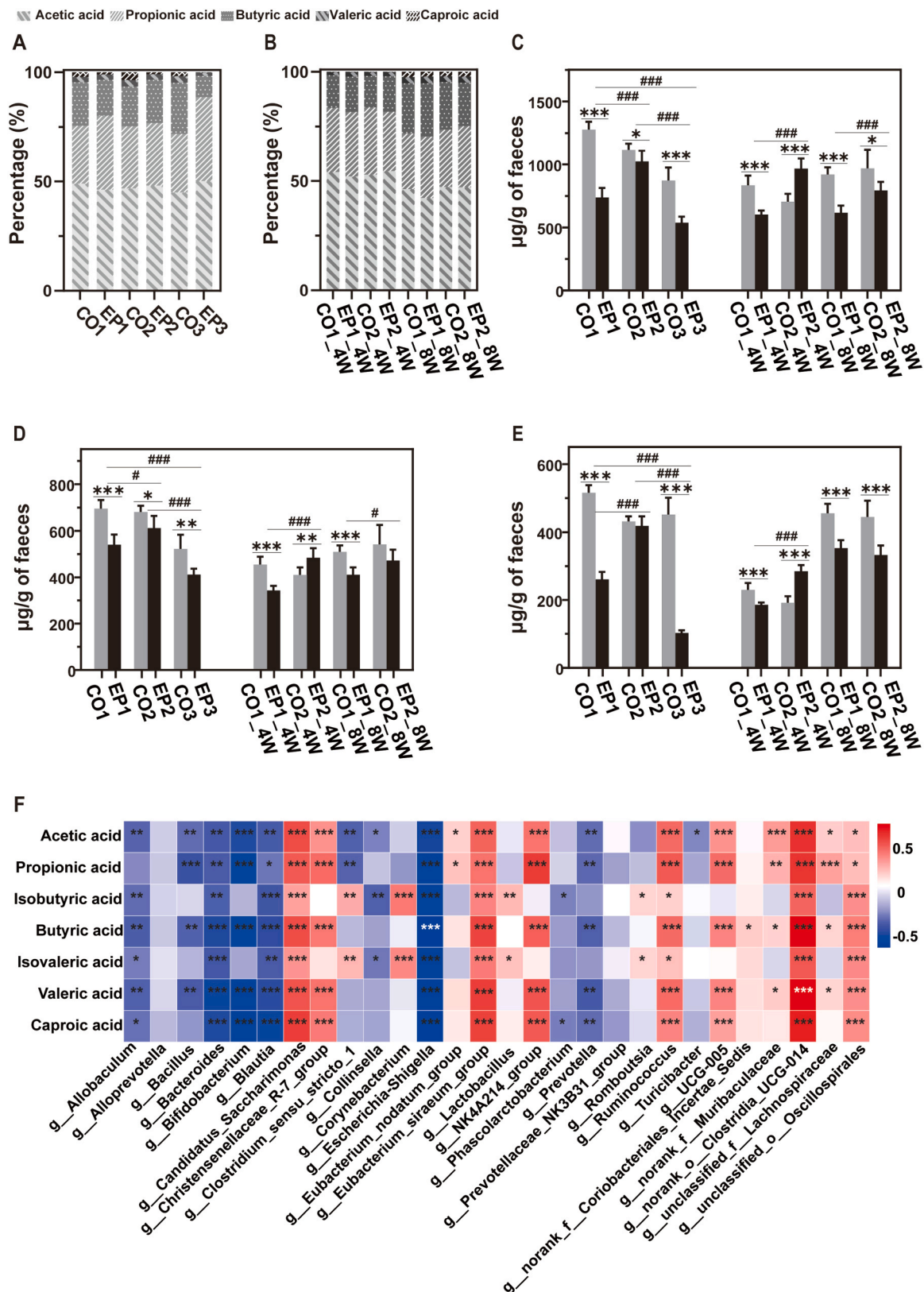


Fig. 4. Percentage composition of major SCFAs in dams and offspring (A, B) (n = 6); Acetic acid levels in dams and offspring (C); Propionic acid levels in dams and offspring (D); Butyric acid levels in dams and offspring (E); Correlation analysis of SCFAs and gut microbiota at the genus level (F). Red denotes positive correlations, while blue denotes negative correlations. (Data presented as means ± SD. * p < 0.05, ** p < 0.01, *** p < 0.001 vs control group; # p < 0.05, ## p < 0.01, *** p < 0.001 vs exposure group).

among which acetate is mainly derived from *Lactobacillus* metabolism, which might contribute to regulating weight control and enhancing insulin sensitivity (Chou et al., 2024). Previous studies have shown that SCFA depletion is associated with metabolic disorders such as obesity and diabetes (Chen et al., 2023; Zhang et al., 2020). Mechanistically, deficient SCFA levels impair intestinal barrier integrity, potentially exacerbating conditions like atopic dermatitis (Xiao et al., 2023). Notably, diabetic patients exhibit characteristic reductions in *norank_o_Clostridia_UCG-014* abundance (Lai et al., 2023), a taxon critical for SCFA biosynthesis. In addition, SCFAs, particularly butyrate, play essential roles in maintaining intestinal epithelial homeostasis and promoting epithelial cell proliferation (Parada Venegas et al., 2019). Their reduction may have impaired intestinal function and was linked to the intestinal alterations observed in this study.

Taken together, the present findings suggested that TCBPA exposure may disrupt gut microbial composition by suppressing key SCFA-producing bacteria, including *Lachnospiraceae*, *Ruminococcus*, *Lactobacillus*, and *norank_o_Clostridia_UCG-014*. Consequently, SCFA levels were reduced in dams and offspring, indicating impaired microbial metabolic function and suggesting a link between microbial dysbiosis and metabolic alterations. This disruption may compromise host metabolic health, although the effects appeared attenuated in adult offspring.

3.5. Influence on the metabolomics of gut microbiota

As depicted in Fig. 5, data points in the QC, control, and exposure groups exhibited strong clustering, indicating stable instrumentation, strong reproducibility, and high data reliability. Stage-specific analyses further demonstrated clear separation between exposed and control groups. In both positive and negative ion modes, the R^2 and Q^2 values exceeded 0.5 and approached 1, indicating robust model reliability and predictive power ($R^2Y = 0.991$ and $Q^2 = 0.986$ for the positive ionization mode and $R^2Y = 0.994$ and $Q^2 = 0.989$ for the negative ionization mode). PLS-DA analysis revealed a distinct separation between TCBPA-exposed and control groups within each developmental stage, suggesting significant TCBPA-induced perturbations in fecal metabolism. These metabolic alterations may be closely associated with disturbances in gut microbial composition observed in this study.

To identify differential metabolites between exposed and control groups, the selection criteria were defined as $p < 0.05$, fold change > 2 or < 0.5 , and $VIP > 1$. Volcano plots (Figs. S4) revealed significant metabolic disturbances in both dams and offspring. A deeper analysis of the metabolic impact of TCBPA exposure showed that dams in the EP1, EP2, and EP3 groups retained 106 common metabolites when compared to their respective controls, with 72, 147, and 167 unique metabolites, respectively (Fig. 5E). In offspring, EP1_4W, EP2_4W, EP1_8W, and EP2_8W groups exhibited only 30 overlapping metabolites, along with 71, 91, 111, and 108 unique metabolites, respectively (Fig. 5F), indicating marked variation in metabolic profiles associated with developmental stage.

KEGG pathway enrichment analysis (MetaboAnalyst) identified 18 significantly altered metabolic pathways ($p < 0.05$) in TCBPA-exposed dams and offspring (Fig. 5 G, S5–6). Among these, arginine and proline metabolism and primary bile acid biosynthesis emerged as key pathways affected across nearly all experimental groups. Notably, similar perturbations in arginine and proline metabolism have been reported by Ye et al. (2016) in TCBPA-exposed marine medaka (*Oryzias melastigma*) embryos, where key intermediates (e.g., proline, ornithine, and citrulline) were significantly altered. Despite differences in experimental models, this consistency suggests that arginine-related metabolism may represent a sensitive target of TCBPA toxicity across species and developmental stages. Furthermore, recent evidence suggests that TCBPA-induced developmental toxicity in nervous and cardiovascular systems may be mediated through arginine-related metabolic disturbances (Liu et al., 2023b).

Arginine metabolism is closely associated with cellular proliferation

and plays a critical role in maintaining intestinal epithelial integrity and barrier function, while also contributing to overall growth and development (Xia et al., 2016; Liu et al., 2023b). Its disruption may contribute to alterations in body weight and intestinal morphology observed in this study (Fig. 1A–F). As a precursor of nitric oxide and polyamines, arginine plays a key role in epithelial renewal, and its disturbance may impair intestinal development. Notably, more pronounced effects were observed in immature offspring (Fig. 1B–C; 1 G), whereas partial recovery was evident in adults (Fig. 1E–F; 1 H), indicating age-dependent susceptibility to TCBPA exposure. In addition, disruption of bile acid metabolism may also contribute to these effects. Bile acids act as important signaling molecules through the farnesoid X receptor (FXR), which regulates intestinal integrity and metabolic homeostasis (Li et al., 2019; Wang et al., 2022). Previous studies have demonstrated that FXR deficiency leads to shortened intestinal villi, whereas its activation promotes villus growth (Yang et al., 2023), and disruption of bile acid availability can induce epithelial apoptosis and reduce villus length (Liu et al., 2018). Therefore, the reduced intestinal length observed in TCBPA-exposed offspring (Fig. 1B–C, E–F) may be mechanistically linked to impaired bile acid–FXR signaling. In addition, FXR also regulates renal metabolic and inflammatory processes, and its dysfunction has been associated with renal injury (Wang et al., 2022). Consistently, the altered kidney weight observed in offspring (Fig. 1G–H) suggests that disruption of bile acid metabolism may contribute to renal physiological changes via FXR-related pathways.

Spearman correlation analysis revealed significant correlations between multiple differential metabolites and genus-level microbiota fluctuations (Figs. 6, S7–9). In dams, *Blautia* abundance was markedly increased in the EP1 group and showed strong positive correlations with 11 metabolites, such as taurine, taurocholic acid, and cholic acid (Fig. S7). This suggests that *Blautia* proliferation may drive elevated levels of these metabolites. Supporting this observation, Ocvirk et al. (2020) reported increased *Blautia* and *Lachnoclostridium* abundance in Alaskan populations with high colorectal cancer incidence, implicating these genera in disease pathogenesis. Notably, both genera belong to the *Lachnospiraceae* family, which is associated with 7α -dehydroxylating bacteria that play a crucial role in bile acid metabolism. Conversely, in the EP3 group, *Eubacterium* exhibited negative correlations with multiple bile acids (e.g., cholic acid, glycocholic acid, and taurocholic acid). This genus, along with *Clostridium*, regulates the activity of 7α -dehydroxylase, a key enzyme involved in converting primary to secondary bile acids, thereby maintaining bile acid homeostasis activity (Jia et al., 2017).

In immature offspring, *Enterococcus* in the CO2_4 W group exhibited significant positive correlations with spermine, gentisic acid, and tyramine, whereas a significant negative correlation was observed with 3-hydroxybutyric acid, spermidine, and gamma-aminobutyric acid (Fig. S8). While *Enterococcus* typically enhances SCFA production and glucose-lipid metabolism, maternal TCBPA exposure appears to have converted it into a pathogenic strain, thereby disrupting offspring metabolism. In adult offspring, the EP1_8 W group exhibited reduced abundance of *norank_f_Ruminococcaceae* and *norank_o_Clostridia_UCG-014*, both of which positively correlated with xanthine, inosine, thymine, and thymidine (Fig. 6). This suggests their depletion may decrease these metabolite levels. Similarly, *Collinsella* abundance was diminished in the EP2_8W group and was positively associated with spermine, 4-hydroxyproline, and proline, key metabolites in arginine and proline metabolism (Fig. S9). The reduction of these metabolites, linked to *Collinsella* depletion, may contribute to renal dysfunction, collagen destabilization, myocardial infarction, and urea cycle disorders (Shan et al., 2022; Xuan et al., 2021).

The present findings from metabolomic analysis demonstrate that TCBPA exposure induces significant dysbiosis in gut microbiota composition while concurrently disrupting microbial metabolic homeostasis. Notably, profound perturbations were observed in key metabolic pathways, including arginine and proline metabolism and bile

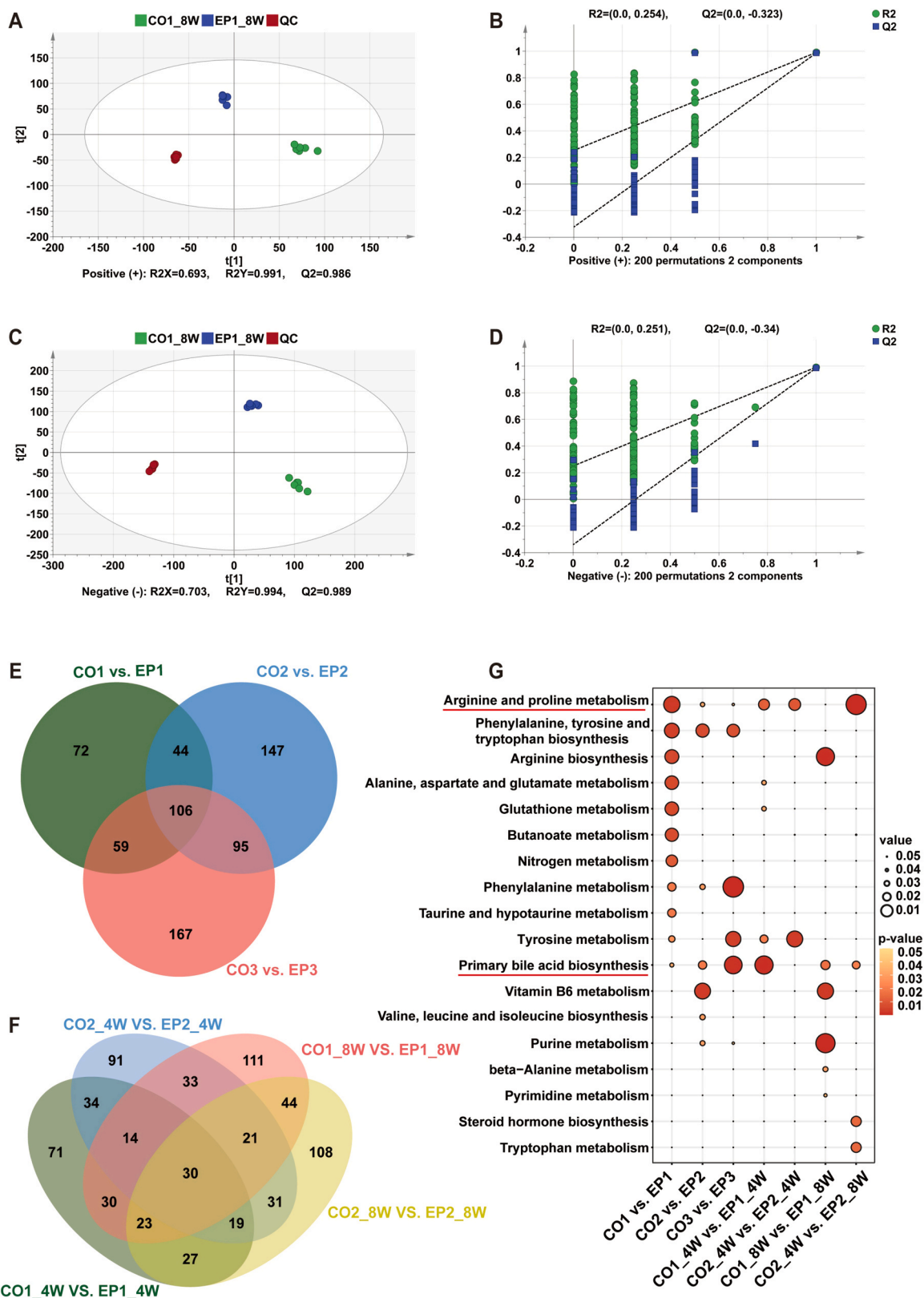


Fig. 5. PLS-DA score plots of metabolomics data in the QC, CO1_8W, and EP1_8W groups in both positive ion mode (A) and negative mode (C) (n = 6). Permutation test of the PLS-DA model in positive ion mode (B) and negative mode (D). Venn diagrams displaying the number of unique and shared metabolites in dams and offspring (E-F). Bubble diagram for metabolic pathway analysis in TCBPA-exposed dams and offspring (G). The size of the counts indicates the value of the different metabolites and the colour indicates the p-value, all less than 0.05.

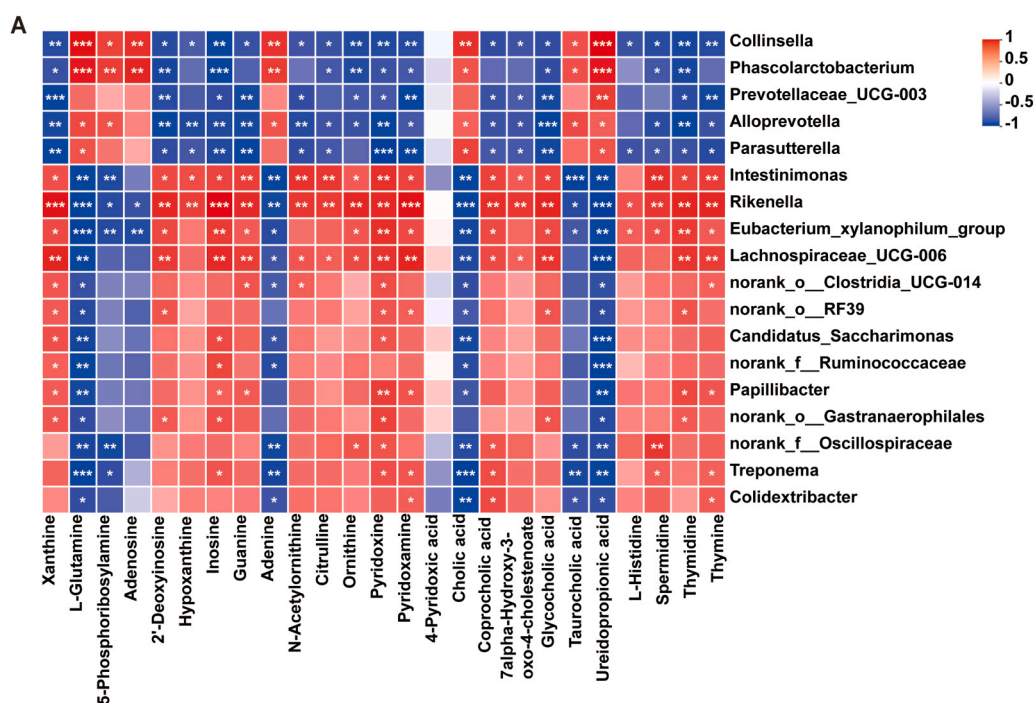


Fig. 6. Association analysis between differential fecal metabolites and the relative abundance of the top 20 bacteria at the genus level in the CO1_8W and EP1_8W groups (n = 6). Red denotes positive correlations, while blue denotes negative correlations. (* $p < 0.05$, ** $p < 0.01$, *** $p < 0.001$ indicate significant differences).

acid biosynthesis. These metabolic disruptions were closely associated with altered abundances of key genera such as *Blautia*, *Eubacterium*, and *Collinsella*. These interdependent changes in microbial ecology and metabolic function may contribute to the observed metabolic disorders, potentially explaining the transgenerational impacts of TCBPA exposure. Together with the SCFA-related changes described above, these coordinated microbiota–metabolite alterations may contribute to the developmental and physiological changes observed in offspring.

3.6. Limitations and perspectives

Because of its lipophilic characteristics and environmental persistence, TCBPA can accumulate in organisms and undergo biomagnification along food chains, potentially contributing to internal exposure in humans and wildlife. Although the experimental dose used in this study exceeds typical human exposure levels, it provides important insights into potential toxicological mechanisms and helps define upper-bound safety thresholds.

Nevertheless, several limitations should be acknowledged. First, the biological functions and causal roles of the identified differential metabolites have not been experimentally validated and require further investigation. Second, only a single exposure dose was applied, limiting the assessment of dose–response relationships. Future studies incorporating multiple dose levels and targeted validation approaches are needed to further elucidate the underlying mechanisms and health implications.

4. Conclusions

This study demonstrates that gestational and/or lactational exposure to TCBPA significantly reduces gut microbial diversity and depletes key SCFA-producing taxa, accompanied by decreased SCFA levels and disruptions in arginine and proline metabolism and primary bile acid biosynthesis. These findings suggest that TCBPA exposure is associated with coordinated alterations in gut microbiota composition and metabolic function, consistent with disruption of the gut microbiota–metabolite axis. The persistence of these changes in offspring

highlights early-life exposure as a sensitive window for microbiome-associated metabolic perturbation. Although the precise mechanisms underlying the interplay between gut microbiota and metabolites remain to be fully elucidated, this study provides evidence for potential intergenerational health effects of TCBPA exposure, particularly in relation to reproductive and developmental toxicity.

CRedit authorship contribution statement

Zhaofa Huang: Data curation. **Yingxin Yu:** Writing – review & editing, Conceptualization. **Chaoyang Long:** Writing – review & editing, Conceptualization. **Yinfeng Zhou:** Writing – original draft, Methodology, Data curation. **Guoxia Zhang:** Methodology. **Zenghua Qi:** Data curation.

Ethics approval

The study was approved the Ethics Review Committee of Southern Medical University (SMUL202403028)

Declaration of Competing Interest

The authors declare that they have no known competing financial interests or personal relationships that could have appeared to influence the work reported in this paper.

Acknowledgments

The study was supported by the Talent Project of Center for Disease Prevention and Control of Guangdong Province (2024D344), the Key R&D Plans of Guangzhou Science and Technology (202206010190), Guangdong Provincial Key R&D Program (2022-GDUT-A0007), and Guangdong-Hong Kong-Macao Joint Laboratory for Contaminants Exposure and Health (2020B1212030008).

Supporting information

Relevant [supplementary material](#) for this article is presented in **Texts S1–S7**, **Table S1**, and **Figs S1–S9**.

Appendix A. Supporting information

Supplementary data associated with this article can be found in the online version at [doi:10.1016/j.ecoenv.2026.120171](https://doi.org/10.1016/j.ecoenv.2026.120171).

Data availability

Data will be made available on request.

References

- Baltazar-Díaz, T.A., González-Hernández, L.A., Aldana-Ledesma, J.M., Peña-Rodríguez, M., Vega-Magaña, A.N., Zepeda-Morales, A.S.M., López-Roa, R.I., del Toro-Areola, S., Martínez-López, E., Salazar-Montes, A.M., Bueno-Topete, M.R., 2022. *Escherichia/Shigella*, SCFAs, and metabolic pathways—the triad that orchestrates intestinal dysbiosis in patients with decompensated alcoholic cirrhosis from Western Mexico. *Microorganisms* 10, 1231. <https://doi.org/10.3390/microorganisms10061231>.
- Beninger, C., Naqvi, S.A., Naushad, S., Orsel, K., Luby, C., Derakhshani, H., Khafipour, E., De Buck, J., 2018. Associations between digital dermatitis lesion grades in dairy cattle and the quantities of four *Treponema* species. *Vet. Res.* 49, 111. <https://doi.org/10.1186/s13567-018-0605-z>.
- Chai, X.Y., Wen, L.Y., Song, Y.Y., He, X.C., Yue, J.X., Wu, J.L., Chen, X., Cai, Z.W., Qi, Z.H., 2023. DEHP exposure elevated cardiovascular risk in obese mice by disturbing the arachidonic acid metabolism of gut microbiota. *Sci. Total Environ.* 875, 162615. <https://doi.org/10.1016/j.scitotenv.2023.162615>.
- Chen, L., Jiang, Q.H., Jiang, C.K., Lu, H.L., Hu, W.J., Yu, S.F., Li, M.Q., Tan, C.P., Feng, Y.C., Xiang, X.W., Shen, G.X., 2023. Sciadonic acid attenuates high-fat diet-induced obesity in mice with alterations in the gut microbiota. *Food Funct.* 14, 2870–2880. <https://doi.org/10.1039/d2fo02524h>.
- Chen, M., Fan, Z.L., Zhao, F.R., Gao, F.M., Mu, D., Zhou, Y.Y., Shen, H., Hu, J.Y., 2015. Occurrence and maternal transfer of chlorinated bisphenol A and nonylphenol in pregnant women and their matching embryos. *Environ. Sci. Technol.* 50, 970–977. <https://doi.org/10.1021/acs.est.5b04130>.
- Chen, X., Li, P., Liu, M., Zheng, H.M., He, Y., Chen, M.X., Tang, W.L., Yue, X.J., Huang, Y.X., Zhuang, L.L., Wang, Z.J., Zhong, M., Ke, G.B., Hu, H.Y., Feng, Y.L., Chen, Y., Yu, Y.H., Zhou, H.W., Huang, L.P., 2020. Gut dysbiosis induces the development of pre-eclampsia through bacterial translocation. *Gut* 69, 513–522. <https://doi.org/10.1136/gutjnl-2019-319101>.
- Chou, X., Fang, M., Shen, Y., Jiang, C.Z., Miao, L., Yang, L.Y., Wu, Z.X., Yao, X.Y., Ma, K.P., Qiao, K., Lin, Z.J., 2024. Ambient PMS pollution, blood pressure, potential mediation by short-chain fatty acids: A prospective panel study of young adults in China. *Ecotoxicol. Environ. Saf.* 287, 117316. <https://doi.org/10.1016/j.ecoenv.2024.117316>.
- Dai, X., Chen, L., Liu, M.Y., Liu, Y., Jiang, S.Q., Xu, T.T., Wang, A.Q., Yang, S.M., Wei, W.H., 2022. Effect of 6-methoxybenzoxazolinone on the cecal microbiota of adult male Brandt's Vole. *Front. Microbiol.* 13, 847073. <https://doi.org/10.3389/fmicb.2022.847073>.
- Dragomirescu, C.C., Lixandru, B.E., Coldea, I.L., Corneli, O.N., Pana, M., Palade, A.M., Cristea, V.C., Suciuc, I., Suciuc, G., Manolescu, L.S.C., Popa, L.G., Popa, M.I., 2020. Antimicrobial susceptibility testing for *Corynebacterium* species isolated from clinical samples in Romania. *Antibiotics* 9, 31. <https://doi.org/10.3390/antibiotics9010031>.
- Gruninger, R.J., Sensen, C.W., McAllister, T.A., Forster, R.J., 2014. Diversity of rumen bacteria in Canadian cervids. *PLoS ONE* 9, e89682. <https://doi.org/10.1371/journal.pone.0089682>.
- Hu, B.H., Liu, S.Q., Luo, Y.Y., Pu, J.Y., Deng, X., Zhou, W.Y., Dong, Y.Q., Ma, Y.C., Wang, G., Yang, F., Zhu, T.H., Zhan, J.S., 2023. Procyanidin B2 alleviates uterine toxicity induced by cadmium exposure in rats: The effect of oxidative stress, inflammation, and gut microbiota. *Ecotoxicol. Environ. Saf.* 263, 115290. <https://doi.org/10.1016/j.ecoenv.2023.115290>.
- Jia, W., Xie, G.X., Jia, W.P., 2017. Bile acid–microbiota crosstalk in gastrointestinal inflammation and carcinogenesis. *Nat. Rev. Gastroenterol. & Hepatol.* 15, 111–128. <https://doi.org/10.1038/nrgastro.2017.119>.
- Lai, Y., Chen, Y.Q., Zheng, J.J., Liu, Z., Nong, D.P., Liang, J.P., Li, Y.B., Huang, Z.H., 2023. Gut microbiota of white-headed black langurs (*Trachypithecus leucocephalus*) in responses to habitat fragmentation. *Front. Microbiol.* 14, 1126257. <https://doi.org/10.3389/fmicb.2023.1126257>.
- Lei, B.L., Yang, Y.X., Xu, L.B., Zhang, X.L., Yu, M.J., Yu, J., Li, N., Yu, Y.X., 2024. Molecular insights into the effects of tetrachlorobisphenol A on puberty initiation in Wistar rats. *Sci. Total Environ.* 911, 168643. <https://doi.org/10.1016/j.scitotenv.2023.168643>.
- Li, M., Wang, Q.S., Niu, M., Yang, H., Zhao, S.M., 2024a. Protective effects of insoluble dietary fiber from cereal bran against DSS-induced chronic colitis in mice: From inflammatory responses, oxidative stress, intestinal barrier, and gut microbiota. *Int. J. Biol. Macromol.* 283, 137846. <https://doi.org/10.1016/j.ijbiomac.2024.137846>.
- Li, S.C., Li, C.L., Wang, W.D., 2019. Bile acid signaling in renal water regulation. *Am. J. Physiol. -Ren. Physiol.* 317, F73–F76. <https://doi.org/10.1152/ajprenal.00563.2018>.
- Li, W.Z., Mu, J., Ni, S.H., Pei, W.L., Wan, L., Wu, X., Zhu, J., Zhang, Z., Li, L., 2024b. Pentachlorophenol exposure delays the recovery of colitis in association with altered gut microbiota and purine metabolism. *Environ. Toxicol.* 40, 101–110. <https://doi.org/10.1002/tox.24420>.
- Li, Z.P., Jin, H., Oh, S.Y., Ji, G.E., 2016. Anti-obese effects of two Lactobacilli and two Bifidobacteria on ICR mice fed on a high fat diet. *Biochem. Biophys. Res. Commun.* 480, 222–227. <https://doi.org/10.1016/j.bbrc.2016.10.031>.
- Lin, S.Y., Zhang, H.N., Wang, C., Su, X.L., Song, Y.Y., Wu, P.F., Yang, Z., Wong, M.H., Cai, Z.W., Zheng, C.M., 2022. Metabolomics reveal nanoplastic-induced mitochondrial damage in human liver and lung cells. *Environ. Sci. & Technol.* 56, 12483–12493. <https://doi.org/10.1021/acs.est.2c03980>.
- Liu, H.L., Bai, Y.X., Yu, Y.Y., Qi, Z.H., Zhang, G.X., Li, G.Y., Yu, Y.X., An, T.C., 2023a. Maternal transfer of resorcinol-bis(diphenyl)-phosphate perturbs gut microbiota development and gut metabolism of offspring in rats. *Environ. Int.* 178, 108039. <https://doi.org/10.1016/j.envint.2023.108039>.
- Liu, R.P., Li, X.J.Y., Huang, Z.M., Zhao, D., Ganesh, B.S., Lai, G.H., Pandak, W.M., Hylemon, P.B., Bajaj, J.S., Sanyal, A.J., Zhou, H.P., 2018. CHOP-induced loss of intestinal epithelial stemness contributes to bile duct ligation-induced cholestatic liver injury. *Hepatology* 67 (4), 1441–1457. <https://doi.org/10.1002/hep.29540>.
- Liu, W.T., Pan, Y.F., Yang, L., Xie, Y., Chen, X.Y., Chang, J., Hao, W.Y., Zhu, L.F., Wan, B., 2023b. Developmental toxicity of TCBA on the nervous and cardiovascular systems of zebrafish (*Danio rerio*): A combination of transcriptomic and metabolomics. *J. Environ. Sci.* 127, 197–209. <https://doi.org/10.1016/j.jes.2022.04.022>.
- Long, D.L., Liu, M., Li, H.Y., Song, J.H., Jiang, X.H., Wang, G., Yang, X.S., 2021. Dysbacteriosis induces abnormal neurogenesis via LPS in a pathway requiring NF- κ B/IL-6. *Pharmacol. Res.* 167, 105543. <https://doi.org/10.1016/j.phrs.2021.105543>.
- Lu, K., Abo, R.P., Schlieper, K.A., Graffam, M.E., Levine, S., Wishnok, J.S., Swenberg, J.A., Tannenbaum, S.R., Fox, J.G., 2014. Arsenic exposure perturbs the gut microbiome and its metabolic profile in mice: an integrated metagenomics and metabolomics analysis. *Environ. Health Perspect.* 122, 284–291. <https://doi.org/10.1289/ehp.1307429>.
- Nair, A.B., Jacob, S., 2016. A simple practice guide for dose conversion between animals and human. *J. Basic Clin. Pharm.* 7, 27–31. <https://doi.org/10.4103/0976-0105.177703>.
- Ocvirk, S., Wilson, A.S., Posma, J.M., Li, J.V., Koller, K.R., Day, G.M., Flanagan, C.A., Otto, J.E., Sacco, P.E., Sacco, F.D., Sapp, F.R., Wilson, A.S., Newton, K., Brouard, F., Delany, J.P., Behnning, M., Appolonia, C.N., Soni, D., Bhatti, F., Methé, B., Fitch, A., Morris, A., Gaskins, H.R., Kinross, J., Nicholson, J.K., Thomas, T.K., O'Keefe, S.J.D., 2020. A prospective cohort analysis of gut microbial co-metabolism in Alaska Native and rural African people at high and low risk of colorectal cancer. *Am. J. Clin. Nutr.* 111, 406–419. <https://doi.org/10.1093/ajcn/nqz301>.
- Parada Venegas, D.P., De la Fuente, M.K., Landskron, G., González, M.J., Quera, R., Dijkstra, G., Harmsen, H.J.M., Faber, K.N., Hermoso, M.A., 2019. Short Chain Fatty Acids (SCFAs)-Mediated Gut Epithelial and Immune Regulation and Its Relevance for Inflammatory Bowel Diseases. *Front. Immunol.* 10, 1486. <https://doi.org/10.3389/fimmu.2019.01486>.
- Reddivari, L., Veeramachaneni, D.N.R., Walters, W.A., Lozupone, C., Palmer, J., Hewaw, M.K.K., Bhatnagar, R., Amir, A., Kennett, M.J., Knight, R., Vanamal, J.K.P., 2017. Perinatal Bisphenol A Exposure Induces Chronic Inflammation in Rabbit Offspring via Modulation of Gut Bacteria and Their Metabolites. *mSystems* 2, e00093-17. <https://doi.org/10.1128/mSystems.00093-17>.
- Rubin, B.S., Murray, M.K., Damassa, D.A., King, J.C., Soto, A.M., 2001. Perinatal exposure to low doses of bisphenol A affects body weight, patterns of estrous cyclicity, and plasma LH levels. *Environ. Health Perspect.* 109, 675–680. <https://doi.org/10.2307/3454783>.
- Shan, M.J., Liu, H., Hao, Y., Song, K.X., Meng, T., Feng, C., Wang, Y.B., Huang, Y.S., 2022. Metabolomic profiling reveals that 5-hydroxylysine and 1-methylnicotinamide are metabolic indicators of keloid severity. *Front. Genet.* 12, 804248. <https://doi.org/10.3389/fgene.2021.804248>.
- Shi, K., Qu, L.H., Lin, X., Xie, Y., Tu, J.Y., Liu, X.Q., Zhou, Z.S., Cao, G.S., Li, S.Q., Liu, Y.J., 2019. Deep-fried *Atractylodes rhizoma* protects against spleen deficiency-induced diarrhea through regulating intestinal inflammatory response and gut microbiota. *Int. J. Mol. Sci.* 21, 124. <https://doi.org/10.3390/ijms21010124>.
- Tu, P.C., Chi, L., Bodnar, W., Zhang, Z.F., Gao, B., Bian, X.M., Stewart, J., Fry, R., Lu, K., 2020. Gut microbiome toxicity: connecting the environment and gut microbiome-associated diseases. *Toxics* 8, 19. <https://doi.org/10.3390/toxics8010019>.
- Wang, H., Wang, D.F., Song, H.X., Ma, X.R., Miao, J.X., Li, J., Yang, W.P., Wang, H.N., 2022. Research progress on the role of gut microbiota dysregulation in the pathogenesis of diabetic nephropathy. *J. Hainan Med. Univ.* 28 (8), 626–634. <https://doi.org/10.13210/j.cnki.jhmu.20201208.002>.
- Wang, J.K., He, Y.T., Yu, D.Q., Jin, L., Gong, X.B., Zhang, B.S., 2020. Perilla oil regulates intestinal microbiota and alleviates insulin resistance through the PI3K/AKT signaling pathway in type-2 diabetic KKAY mice. *Food Chem. Toxicol.* 135, 110965. <https://doi.org/10.1016/j.fct.2019.110965>.
- Wei, X.J., Yang, D.Q., Zhang, B.Y., Fan, X.P., Du, H.N., Zhu, R.J., Sun, X.T., Zhao, M.M., Gu, N., 2022. Di-(2-ethylhexyl) phthalate increases plasma glucose and induces lipid metabolic disorders via FoxO1 in adult mice. *Sci. Total Environ.* 842, 156815. <https://doi.org/10.1016/j.scitotenv.2022.156815>.
- Xia, M., Ye, L.L., Hou, Q.H., Yu, Q.H., 2016. Effects of arginine on intestinal epithelial cell integrity and nutrient uptake. *Br. J. Nutr.* 116, 1675–1681. <https://doi.org/10.1017/S000711451600386X>.

- Xiao, X.J., Hu, X.S., Yao, J.P., Cao, W., Zou, Z.H., Wang, L., Qin, H.Y., Zhong, D.L., Li, Y. X., Xue, P.W., Jin, R.J., Li, Y., Shi, Y.Z., Li, J., 2023. The role of short-chain fatty acids in inflammatory skin diseases. *Front. Microbiol.* 13. <https://doi.org/10.3389/fmicb.2022.1083432>.
- Xuan, C., Li, H., Tian, Q.W., Guo, J.J., He, G.W., Lun, L.M., Wang, Q., 2021. Quantitative assessment of serum amino acids and association with early-onset coronary artery disease. *Clin. Interv. Aging* 16, 465–474. <https://doi.org/10.2147/cia.S298743>.
- Yang, J.F., van Dijk, T.H., Koehorst, M., Havinga, R., de Boer, J.F., Kuipers, F., van Zutphen, T., 2023. Intestinal Farnesoid X receptor modulates duodenal surface area but does not control glucose absorption in mice. *Int. J. Mol. Sci.* 24, 4132. <https://doi.org/10.3390/ijms24044132>.
- Yao, Z., Tao, S.H., Lai, Y.J., Yu, Y., Wang, H., Sang, J.M., Yang, J., Li, H.T., Li, X.H., Li, Y., Ning, Y.Y., Ge, R.S., Li, S.J., 2024. The impact of tetrachlorobisphenol A exposure during puberty: Altered Leydig cell development and induced endoplasmic reticulum stress in male mice. *Ecotoxicol. Environ. Saf.* 270, 115895. <https://doi.org/10.1016/j.ecoenv.2023.115895>.
- Ye, G.Z., Chen, Y.J., Wang, H.O., Ye, T., Lin, Y., Huang, Q.S., Chi, Y.L., Dong, S.J., 2016. Metabolomics approach reveals metabolic disorders and potential biomarkers associated with the developmental toxicity of tetrabromobisphenol A and tetrachlorobisphenol A. *Sci. Rep.* 6, 35257. <https://doi.org/10.1038/srep35257>.
- Zha, X., Elsabagh, M., Zheng, Y., Zhang, B., Wang, H.R., Bai, Y.L., Zhao, J.W., Wang, M. Z., Zhang, H., 2024. Impact of Bisphenol A exposure on maternal gut microbial homeostasis, placental function, and fetal development during pregnancy. *Reprod. Toxicol.* 129, 108677. <https://doi.org/10.1016/j.reprotox.2024.108677>.
- Zhang, G.X., Ren, Q.Q., Ma, S.T., Wu, J.G., Yang, X.F., Yu, Y.X., 2020. Intergenerational transfer of Dieldrin Plus and the associated long-term effects on the structure and function of gut microbiota in offspring. *Environ. Int.* 141, 105770. <https://doi.org/10.1016/j.envint.2020.105770>.
- Zhang, G.X., Ma, F.M., Zhang, Z.W., Qi, Z.H., Luo, M.Q., Yu, Y.X., 2023. Associated long-term effects of decabromodiphenyl ethane on the gut microbial profiles and metabolic homeostasis in Sprague-Dawley rat offspring. *Environ. Int.* 172, 107802. <https://doi.org/10.1016/j.envint.2023.107802>.
- Zhang, H.J., Liu, W.L., Chen, B., He, J.B., Chen, F.F., Shan, X.D., Du, Q.X., Li, N., Jia, X. Y., Tang, J., 2018. Differences in reproductive toxicity of TBBPA and TCBPA exposure in male *Rana nigromaculata*. *Environ. Pollut.* 243, 394–403. <https://doi.org/10.1016/j.envpol.2018.08.086>.
- Zhuang, M., Shang, W.T., Ma, Q.C., Strappe, P., Zhou, Z.K., 2019. Abundance of probiotics and butyrate-production microbiome manages constipation via short-chain fatty acids production and hormones secretion. *Mol. Nutr. Food Res.* 63, 1801187. <https://doi.org/10.1002/mnfr.201801187>.